

# Static Recrystallization of Cold Rolled Intermetallic Fe17Al4Cr0.3Zr Alloy

P. Kratochvíl, I. Schindler, P. Hanus, R. Král, and P. Hrcuba

(Submitted May 13, 2011; in revised form November 26, 2011)

The final microstructure of cold rolled intermetallic disordered alloy Fe17Al4Cr0.3Zr was rebuilt during the annealing at moderate temperatures in the range of 800 to 900 °C. The time necessary to obtain recrystallized structure was determined at several annealing temperatures to optimize the processing technology of the plates. The phases present in the material during this process were identified. The grain growth (grain boundary movement) during static recrystallization (SRX) is connected with the interaction with an array of the Laves phase  $\lambda_1(\text{Fe,Al})_2\text{Zr}$  and ZrC particles. The Avrami-based phenomenological model describing kinetics of SRX was developed. The activation energy for recrystallization was estimated.

**Keywords** cold rolled alloy, Fe-Al alloy, precipitates, static recrystallization

## 1. Introduction

Two phases, Fe<sub>3</sub>Al and FeAl, have recently been investigated as potential structural materials. This is valid as well for the intermetallic materials with disordered structure containing <20 at.% Al. A great advantage of these materials may be mainly low density and high chemical resistance at high temperatures; therefore, these materials represent a growing subject of interest in the field of the high-temperature applications.

The important technology used as the initial processing of casts of Fe-Al alloys is the hot rolling. The rolling takes place mostly at the temperatures at which these alloys are disordered and hence the deformation behaviour is the function of Al content in the A2 lattice. The situation can be modified by additives (either as solutes or as phases). It is possible to recover the structure by static recrystallization (SRX) for the repeated rolling quickly by intermediate pass heating. The efficiency of the annealing (time and temperature) after cold rolling (structure with elongated grains) is important. The rolling and SRX of Fe<sub>3</sub>Al type alloys are described, e.g., in Ref 1-4. Scant information for the disordered (ferritic) alloy (Al content lower as 20 at.%) is available at present in Ref 5, 6.

The phase that appears in Fe-Al materials low alloyed by Zr is Laves phase  $\lambda_1(\text{Fe,Al})_2\text{Zr}$ , see Ref 7, 8. This is due to the fact that Zr is not soluble in Fe-Al alloys (see ternary phase

diagram Fe-Al-Zr, Ref 7) (Fig. 1). The prior formation of ZrC is connected with the affinity of C to Zr and to the presence of carbon in the raw iron used for the preparation of alloys (Ref 9).

For the economy of the rolling process the low finishing temperatures as well as the low annealing temperatures to recover the material before the next pass or for any technological operation are important. The influence of rolling temperature on the structure resulting by the multi-pass laboratory rolling of ferritic disordered intermetallic alloy is given in Ref 10. It is the purpose of this article to describe the structure of such alloy after low finish rolling temperature and the subsequent recrystallization during annealing process.

## 2. Experimental Procedure

The actual composition of the studied material was determined by spectral and by carbon combustion analysis is (at.%): Fe–17.3 Al–3.8 Cr–0.3 Zr–0.13 C. The laboratory castings were prepared by the vacuum melting. They were heated at 1200 °C, hot rolled with 7 reverse height reductions from initial thickness of 20 mm to final thickness of 3.2 mm and cooled free on air. During the even inter-pass intervals, the rolled specimens were additionally heated. Due to very high deformation resistance values, the specimens have to be heated to temperature 700 °C before the subsequent cold forming (i.e., under the temperature of SRX). The cold rolling was realized in laboratory four-high rolling mill (working rolls with diameter 67 mm, circumferential velocity 70 rpm) with one relative height reduction 37 % (final thickness 2.0 mm). The final microstructure of the cold formed plates was fixed by oil quenching immediately after rolling. For the study of SRX smaller specimens were taken from the rolled plates and annealed at temperatures between 800 and 1000 °C to reach the recrystallized state.

The structure was studied, using the methods as follows:

- X-ray diffraction (XRD) for the phase identification.
- Light optical microscopy (LOM)—the specimens were studied in the vertical section parallel to the direction of

**P. Kratochvíl, R. Král, and P. Hrcuba**, Department of Material Physics, Faculty of Mathematics and Physics, Charles University, Ke Karlovu 5, 12116 Prague 2, Czech Republic; **I. Schindler**, Faculty of Metallurgy and Materials Engineering, VSB—Technical University of Ostrava, 17. Listopadu 15, 70833 Ostrava, Czech Republic; and **P. Hanus**, Department of Material Science, Faculty of Mechanical Engineering, Technical University of Liberec, Hálkova 6, 46117 Liberec, Czech Republic. Contact e-mail: pektrat@met.mff.cuni.cz.

rolling. Polishing and etching by emulsion OP-S (Struers) and subsequently 100 mL H<sub>2</sub>O + 40 mL HNO<sub>3</sub> + 15 mL HCl solution was applied.

- Transmission electron microscopy (TEM) and selected area electron diffraction (SAED)—the foils were prepared by electro-discharge machining (EDM) and electrolytic double jet polishing at -40 °C, using 10% solution of HNO<sub>3</sub> in methanol.
- To make the high-angle grain boundaries visible, specimens were analyzed by the scanning electron microscopy with the back-scattered diffraction (EBSD). 20 kV accelerating voltage was used. Scans were captured with 0.5 μm step size. Single iterative grain dilatation procedure was used for cleaning raw data. The individual grains with the disorientation 10° and more were distinguished.
- The volume fraction was evaluated by software NIS Elements 3.1. The recrystallized volume fraction ( $X_v$ ) was determined with use of the classifier based on Bayes decision tree (shape factor, circularity, and area of each grain). The turn frame was 500 μm below the surface and area of turn frame was 470 × 400 μm.

### 3. Experimental Results

The recrystallized volume fraction ( $X_v$ ) of the original cold formed sample is smaller as 2.0%. The deformed grains elongated in the direction of rolling are obvious in Fig. 2.

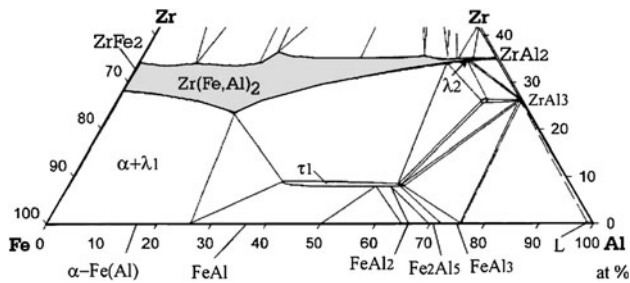


Fig. 1 Fe-Al-Zr phase diagram for 800 °C (Ref 7)

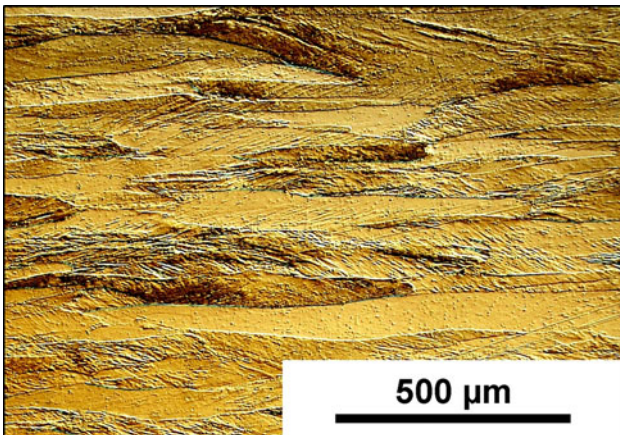


Fig. 2 The structure of the cold rolled material

The phases in tested rolled material were identified as ZrC and Laves phase  $\lambda_1$  (Fe,Al)<sub>2</sub>Zr. ZrC is formed due to the strong bond Zr-C. The rest of Zr forms (Fe,Al)<sub>2</sub>Zr. These phases take place in the SRX. Both tiny ZrC particles of with size up to 50 nm and coarse particles of (Fe,Al)<sub>2</sub>Zr with size 1-2 μm influence dislocations movement through the matrix (Fig. 3) and the migration of the grain boundaries (Fig. 4) during SRX. The temperature 950 °C and higher led to a too fast increase of recrystallized volume. A massive nucleation of new grains occurred, especially on the boundaries of the original grains. The SRX at 950 and 1000 °C was completed after <1 min. Therefore, the temperatures 800, 850, and 900 °C were chosen for further tests. The results of the determination of  $X_v$  as a function of annealing temperature and time are in Table 1. The SRX process is illustrated in Fig. 5.

Notice: Pictures presented in Fig. 5(a) to (d) do not show orientation maps. Every grain has random color which has no relation to its orientation. Criterion for coloring certain grain is just the 10° limit for high-angle grain boundaries. Between grains on the picture are high-angle boundaries. Low-angle boundaries are not visible on this type of picture.

The process at 800 °C is very slow (Fig. 5a, b), characterized by small nuclei. The small features formed in Fig. 5(a) are nuclei appearing in the grain deformation inhomogeneities and along grain boundaries. Exceptionally is the size of the mentioned features so small that it is comparable with the

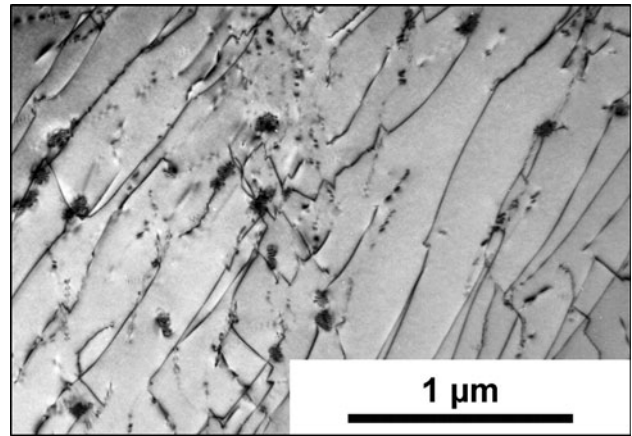


Fig. 3 Pinning of dislocations by particles of ZrC

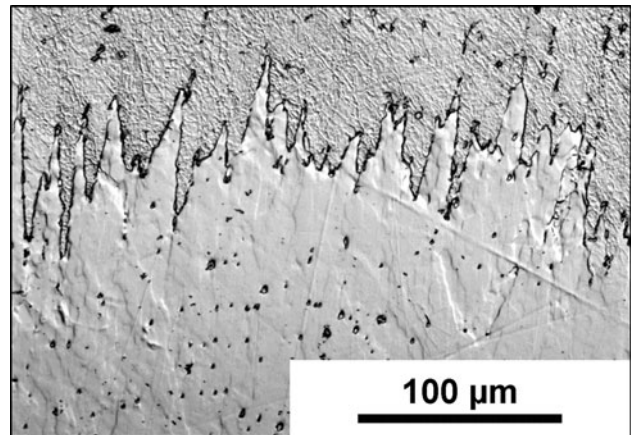


Fig. 4 Pinning of grain boundaries by particles of (Fe,Al)<sub>2</sub>Zr

Laves phase particles (compare with particles in Fig. 4). Further SRX process at 850 °C and its finishing at 900 °C is presented in Fig. 5(c) and (d), respectively.

In general, it was possible to refine the grain size by recrystallization annealing after the cold rolling more effectively as compared with the annealing after high temperature finishing (Ref 5).

#### 4. Discussion

SRX is a key issue for both cold and hot rolling for metals and alloys. The softening process essentially decreases the forming forces and determines the resulting microstructure and therefore the mechanical properties of the finished sheets. The

**Table 1 Recrystallized volume fraction as a function of annealing temperature and time**

800 °C		850 °C		900 °C	
<i>t</i> , s	<i>X<sub>v</sub></i> , %	<i>t</i> , s	<i>X<sub>v</sub></i> , %	<i>t</i> , s	<i>X<sub>v</sub></i> , %
600	6.0	120	7.5	60	13.6
1200	17	240	24	180	50
1800	21	360	26	360	78
2400	31	960	60	720	93

models describing the kinetics of the static recrystallization are used for the prediction of parameters of the rolling and cooling especially for the determination of proper correlation of the temperature and time of the annealing after the forming.

The static recrystallization process of the cold-rolled disordered intermetallic Fe17Al4Cr0.3Zr is governed by nucleation process and by the movement of grain boundaries of new grains through the arrangement of Laves phase  $\lambda_1$  (Fe,Al)<sub>2</sub>Zr and ZrC particles. The volume fractions of both types of obstacles are the function first of the concentration of Zr and C. The ratio of both concentrations determines the number and size of both types of obstacles. The conclusions about the temperatures and times of the recrystallization annealing valid for the tested alloy cannot be therefore applied to Fe-Al alloys with compositions different from the present one. The only way to handle the problem is presented here.

We assume that the process of static recrystallization in this study can be described in the terms of the Johnson, Mehl, Avrami and Kolmogorov (JMAK) model (Ref 11-13).

In case of homogeneous distribution of stored deformation energy and random distribution of nuclei, the recrystallization kinetics is given by

$$X_v(t) = 1 - \exp(-B \cdot t^n) \quad (\text{Eq 1})$$

where *t* (s) is annealing time. The constant *B* depends on the mechanisms of nucleation and growth, and *n* is an Avrami exponent, for details see, e.g., Ref 14.

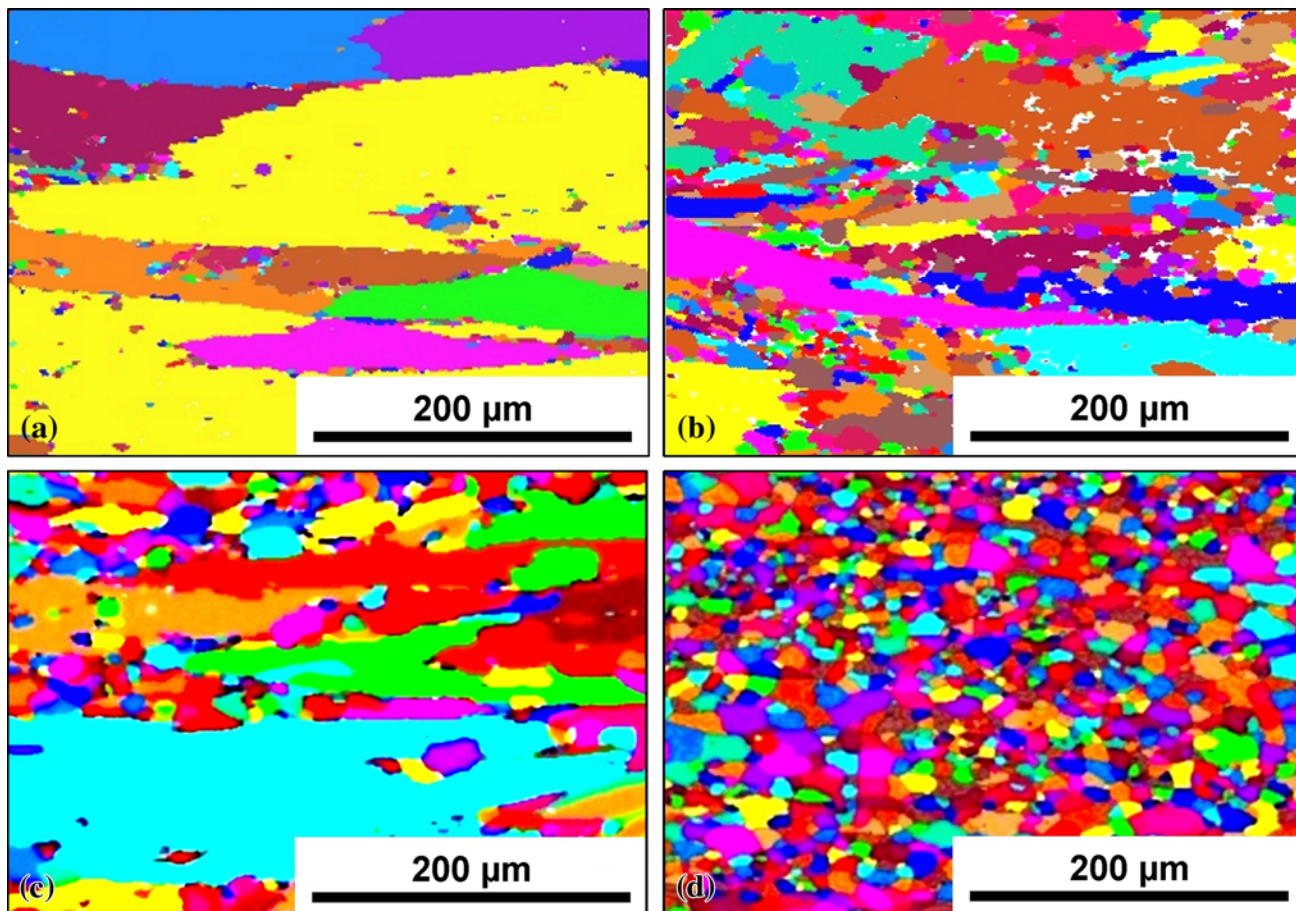


**Fig. 5** The structure of the selected samples (EBSD). (a) Annealed 600 s at 800 °C, (b) annealed 2400 s at 800 °C, (c) annealed 360 s at 850 °C, and (d) annealed 720 s at 900 °C

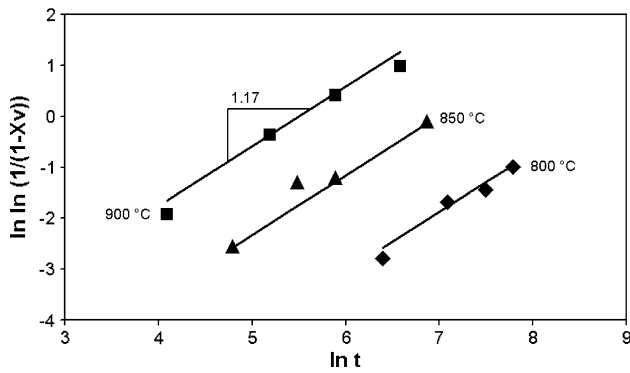


Fig. 6 Determination of Avrami exponent from experimental data (Table 1) by regression analysis

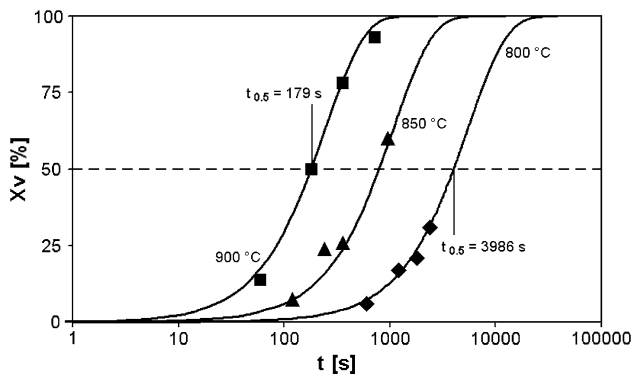


Fig. 7 Kinetics of SRX: curves—Eq 2, squares—experimental data

The coefficients in Eq 1 were evaluated by multiple nonlinear regression on data in Table 1 using statistics software UNISTAT 5.6. Independent variables were the temperature  $T$  and the time of annealing  $t$ . The average value of the Avrami exponent  $n = 1.17$  (see Fig. 6).

The effect of the temperature of annealing was introduced into Eq 1 by a modification of the quantity  $B$ . The resulting equation of the phenomenological model describing the kinetics of SRX of the tested alloy is

$$X_v(T, t) = 1 - \exp \left[ -1.4 \cdot 10^{14} \cdot \exp \left( \frac{-45779}{T} \right) \cdot t^{1.17} \right] \quad (\text{Eq 2})$$

where  $T$  (K) is the annealing temperature. Good agreement of experimental values with values obtained using Eq 2 is obvious in Fig. 7.

If we consider the SRX process as a whole, we can take the time  $t_{0.5}$  (s) necessary for  $X_v = 50\%$  as a measure of the rate of recrystallization. From the measurements of time  $t_{0.5}$  for two different temperatures  $T_1$  and  $T_2$  we can evaluate the activation energy  $Q$  as follows, see e.g., Ref 15

$$Q = -R \cdot \frac{\ln t_{0.5(1)} - \ln t_{0.5(2)}}{T_2^{-1} - T_1^{-1}} \quad (\text{Eq 3})$$

The value of  $t_{0.5}$  using experimental data and Eq 2 is 3986 s for 800 °C and 179 s for 900 °C. Substituting to Eq 3, the evaluated activation energy  $Q = 325$  kJ/mol which is higher than  $Q = 260$  kJ/mol found for Fe-24at.%Al (Ref 16) in temperature range 850-1050 °C. This difference may be due to

the effect of Zr-rich particles (obstacles). From the extrapolation of experimental data, the time necessary for the complete recrystallization (taken as  $X_v = 95\%$ ) can be estimated to be ca 10 and 45 min for the annealing temperatures 900 and 850 °C, respectively. In case of annealing at 800 °C the process of SRX is very slow, resulting in  $X_v = 32\%$  after 40 min of annealing.

Rather long time periods are necessary to complete SRX of the tested alloy at temperature lower than 900 °C. These are hardly compatible with the possibilities of additional annealing during interpass intervals in the conditions of hot rolling mills. It is verified that it is appropriate to choose the higher rolling temperatures (Ref 10).

Equation 2 makes it possible to determine the recrystallized volume fraction for the tested alloy as a function of temperature at isothermal hold. It is therefore useful to adjust the final thermal treatment after cold rolling.

## 5. Conclusions

1. SRX was investigated at temperatures 800-900 °C for the disordered intermetallic Fe–17.3 Al–3.8 Cr–0.3 Zr–0.13 C (at.%) alloy.
2. SRX is influenced by the presence of zirconium carbide ZrC and Laves phases  $(\text{Fe,Al})_2\text{Zr}$  particles.
3. For the description of SRX, an Avrami-based phenomenological model is developed.
4. The activation energy  $Q = 325$  kJ/mol in the temperature range 800-900 °C.

## Acknowledgments

The authors acknowledge the financial support of Ministry of School of the Czech Republic (the project No. 6198910015), of the Grant Agency of the Czech Republic (the project No. 106/08/1238) and of the operation program “Research and Development for Innovations” financed by the Structural Funds and by the state budget of the Czech Republic (the project No. CZ.1.05/2.1.00/01.0040).

## References

1. Y.D. Huang and L. Froyen, Recovery, Recrystallization and Grain Growth in Fe<sub>3</sub>Al-Based Alloys, *Intermetallics*, 2002, **10**, p 473–484
2. J. Konrad, S. Zaefferer, A. Schneider, D. Raabe, and G. Frommeyer, Hot Deformation Behavior of a Fe<sub>3</sub>Al-Binary Alloy in the A2 and B2-Order Regimes, *Intermetallics*, 2005, **13**, p 1304–1312
3. P. Kratochvil and I. Schindler, Conditions for Hot Rolling of Iron Aluminide, *Adv. Eng. Mater.*, 2004, **6**, p 307–310
4. P. Kratochvil and I. Schindler, Hot Rolling of Iron Aluminide Fe<sub>28.4</sub>Al<sub>14.1</sub>Cr<sub>0.02</sub>Ce (at.%), *Intermetallics*, 2006, **8**, p 436–438
5. P. Kratochvil, I. Schindler, P. Hanus, and P. Suchanek, Structure of Rolled Ferrite Alloyed with 9.3 wt.% Al and 0.5 wt.% Zr, *Kovove Mater.*, 2008, **46**, p 257–261
6. R.G. Baligidad and A. Radhakrishna, Effect of Zirconium on Structure and Properties of High Carbon Fe-10.5 wt-%Al Alloy, *Mater. Sci. Technol.*, 2004, **20**, p 111–116
7. F. Stein, M. Palm, and G. Sauthoff, Mechanical Properties and Oxidation Behaviour of Two-Phase Iron Aluminium Alloys with Zr(Fe,Al)<sub>2</sub> Laves Phase or Zr(Fe,Al)<sub>12</sub> τ<sub>1</sub> Phase, *Intermetallics*, 2005, **13**, p 1275–1285
8. A. Wasilkowska, M. Bartsch, F. Stein, M. Palm, G. Sauthoff, and U. Messerschmidt, Plastic Deformation of Fe-Al Polycrystals Strengthened with Zr-Containing Laves Phases—Part II. Mechanical Properties, *Mat. Sci. Eng. A*, 2004, **381**, p 1–15

9. M. Cieslar and M. Karlík, Carbide Formation in Zr-Containing Fe<sub>3</sub>Al-Based Alloys, *Mater. Sci. Eng. A*, 2007, **462**, p 289–293
10. I. Schindler, P. Kratochvíl, P. Hanus, and P. Kozelský, Hot Rolling and Deformation Behavior of Fe<sub>17</sub>Al<sub>4</sub>Cr<sub>0.3</sub>Zr Alloy, *High Temp. Mater. Process.*, 2010, **29**, p 19–25
11. W.A. Johnson and R.F. Mehl, Reaction Kinetics in Processes of Nucleation and Growth, *Trans. AIME.*, 1939, **135**, p 416–442
12. M. Avrami, Kinetics of Phase Change, *J. Chem. Phys.*, 1939, **7**, p 1103–1112
13. A.N. Kolmogorov, On the Statistical Theory of Metal Crystallization (in Russian), *Izv. Akad. Nauk SSSR Ser. Matem.*, 1937, **3**, p 355–359
14. F.J. Humphreys and M. Hatherly, *Recrystallization and Related Annealing Phenomena*, Pergamon Press, Oxford, 2002, p 173–233
15. S. Wang, S.B. Kang, and J.H. Cho, Effect of Hot Compression and Annealing on Microstructure Evolution of ZK60 magnesium alloys, *J. Mater. Sci.*, 2009, **44**, p 5475–5484
16. Y.V.R.K. Prasad, D.H. Sastry, R.S. Sundar, and S.C. Deevi, Optimization of Hot Workability and Hot Deformation Mechanisms in FeAl and Fe<sub>3</sub>Al Based Alloys, *Structural Intermetallics*, K.J. Hemker, D.M. Dimiduk, H. Clemens, R. Darolia, H. Inui, and J.M. Larsen, Ed., Sept 23–25, 2001 (Jackson hole), TMS, 2001, p 233–239